Coexistence of Quantized, Time Dependent, Clusters in Globally Coupled Oscillators

Hongjie Bi,[1] Xin Hu,[2] S. Boccaletti,[3,4,*] Xingang Wang,[5] Yong Zou,[1] Zonghua Liu,[1] and Shuguang Guan[1,†]
[1]Department of Physics, East China Normal University, Shanghai 200241, China
[2]Suzhou Institute of Nano-Tech and Nano-Bionics, Chinese Academy of Sciences, Suzhou 215123, China
[3]CNR-Institute of Complex Systems, Via Madonna del Piano, 10, 50019 Sesto Fiorentino, Florence, Italy
[4]The Embassy of Italy in Tel Aviv, 25 Hamered Street, 68125 Tel Aviv, Israel
[5]School of Physics and Information Technology, Shaanxi Normal University, Xian 710062, China
(Received 13 November 2015; revised manuscript received 17 September 2016; published 10 November 2016)

We report on a novel collective state, occurring in globally coupled nonidentical oscillators in the proximity of the point where the transition from the system's incoherent to coherent phase converts from explosive to continuous. In such a state, the oscillators form quantized clusters, where neither their phases nor their instantaneous frequencies are locked. The oscillators' instantaneous speeds are different within the clusters, but they form a characteristic cusped pattern and, more importantly, they behave periodically in time so that their average values are the same. Given its intrinsic specular nature with respect to the recently introduced Chimera states, the phase is termed the *Bellerophon* state. We provide an analytical and numerical description of *Bellerophon* states, and furnish practical hints on how to seek them in a variety of experimental and natural systems.

DOI: 10.1103/PhysRevLett.117.204101

The emergence of coherent phases of interacting oscillators is one of the most important phenomena in nature, and is the foundation for the cooperative functioning of a wealth of different systems. To gather understanding on the mechanisms underlying such organizational behavior, physicists resort to solvable and simplified frameworks, such as the Kuramoto [1] and Kuramoto-like [2–4] models, where a variety of collective states can be described: from full [5,6], to cluster [7,8], to explosive synchronization (ES) [4,9]. Recently, various types of Chimera states (CSs) (the coexistence of coherent and incoherent domains, which occurs, remarkably, for fully identical locally coupled oscillators) [10,11] have been described and observed in experiments [12], including the breathing CS [13], the clustered CS [14], and the multi CS [15].

In this Letter we report on a previously unknown coherent phase that is proper, instead of globally coupled oscillators with widely different frequencies, and which emerges in the proximity of the parameter point where the transition from the system's incoherent to coherent behavior converts from explosive to continuous. In the novel state, the oscillators form quantized clusters, where neither their phases nor their instantaneous frequencies are locked. Each of the oscillators' instantaneous speeds is different within the clusters, but the instantaneous frequencies form the same cusped pattern characterizing the average speeds of CS. The oscillators's instantaneous frequencies behave periodically in time so that their average values are the same. Because of its intrinsic specular nature with respect to CS, the new phase is termed here the *Bellerophon* state, as *Bellerophon* was the great hero who, in Greek mythology, confronted the monster Chimera [16].

We start assuming the framework of a Kuramoto-like model of N globally coupled phase oscillators, which reads

$$\dot{\theta}_i = \omega_i + \frac{\kappa_i}{N}\sum_{j=1}^{N}\sin(\theta_j - \theta_i), \qquad i = 1, \ldots, N, \quad (1)$$

where the dots denote temporal derivatives and θ_i, ω_i, and κ_i are the instantaneous phase, the natural frequency, and the coupling strength of the ith oscillator, respectively. The level of synchronization is measured by the order parameter $R = \frac{1}{N}\langle|\sum_{j=1}^{N} e^{i\theta_j}|\rangle_T$, where $|\cdot|$ and $\langle\cdot\rangle_T$ denote the module and time average, respectively. The set of natural frequencies $\{\omega_i\}$ is drawn from a given frequency distribution (FD) $g(\omega)$. In the following, two distinct cases will be illustrated, which have in common the fact that they sustain both a first- and a second-order-like transition to synchronization; i.e., the coherent phase may occur (for proper parameter choices) abruptly. Namely, case (1) corresponds to setting $\kappa_i = \kappa|\omega_i|$, i.e., to establishing a correlation between the oscillator's natural frequency and the coupling strength; case (2) considers instead two distinct populations of oscillators (conformists and contrarians) [17]), i.e., with κ_i only taking two values (either $\kappa_1 < 0$ or $\kappa_2 > 0$).

For the sake of illustration, let us start from case (1), and with a FD that is assumed to be an even function $[g(\omega) = g(-\omega)]$, symmetric, and centered at zero. We take $g(\omega) = \frac{\Delta}{2\pi}[(1/(\omega-\omega_0)^2 + \Delta^2) + (1/(\omega+\omega_0)^2 + \Delta^2)]$ to be a bimodal Lorentzian distribution, where Δ is the width parameter (half width at half maximum) of each Lorentzian and $\pm\omega_0$ are their center frequencies. Notice that, depending on ω_0/Δ, such a FD can be, in fact, either unimodal

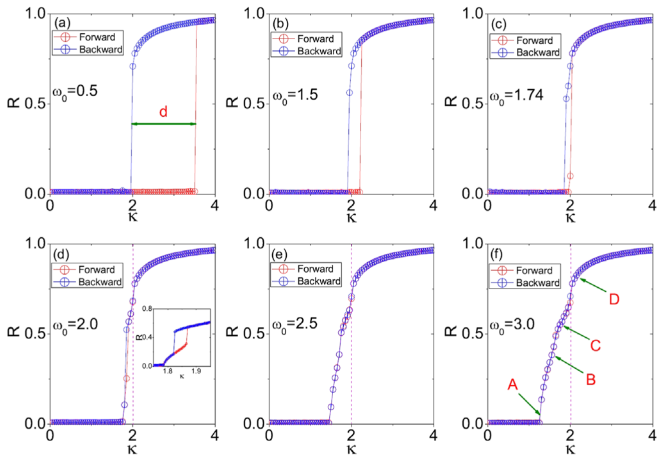

FIG. 1. From an explosive to a continuous transition. R vs κ for model (1). $\Delta = 1$ and $\omega_0 = 0.5$ (a), 1.5 (b), 1.74 (c), 2.0 (d), 2.5 (e), and 3.0 (f).

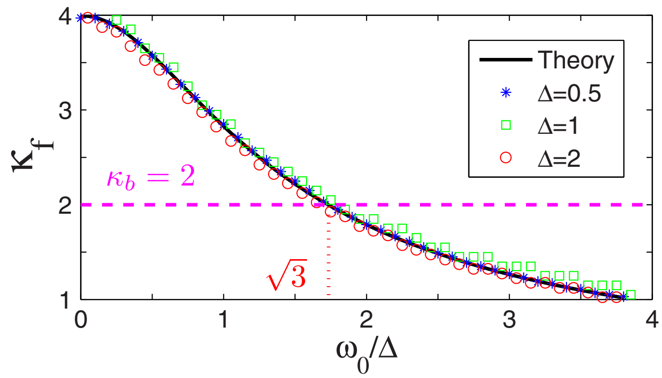

FIG. 2. Critical point for the forward transition. κ_f vs ω_0/Δ. The black curve corresponds to the analytic solution (see the Supplemental Material [19] for details). The purple dashed line marks the backward transition point. The theoretical prediction and the numerical results coincide perfectly.

($\omega_0/\Delta \le \sqrt{3}/3$) or bimodal ($\omega_0/\Delta > \sqrt{3}/3$). We first investigate numerically the synchronization transition in system (1). As the considered FD has two basic parameters (ω_0 and Δ), we fix for simplicity $\Delta = 1$ and let ω_0 increase (which, physically, is tantamount to progressively increasing the distance between the two peaks of the FD). The results are shown in Fig. 1 [18]. For small values of ω_0, an irreversible, first-order-like, abrupt transition [Fig. 1(a)] is observed, featuring a characteristic hysteresis area whose width can be defined as $d = \kappa_b - \kappa_f$ (with κ_b and κ_f being the critical points for the backward and forward transitions, respectively). Figures 1(b) and 1(c) show that the width of the hysteresis area progressively shrinks as ω_0 increases. Eventually, when ω_0 is large enough [Figs. 1(d)–1(f)], one observes a reversible, second-order-like transition.

As long as the FD is symmetric (as in the present case), the critical point for the backward transition is $\kappa_b = 2$ [3], which is fully verified in our simulations [see Figs. 1(a)–1(c)]. However, the critical point κ_f for the forward transition actually varies with ω_0 (at $\Delta = 1$), thus inducing the hysteresis area to shrink, and leading eventually to the observed conversion from an ES to a continuous transition to synchronization (occurring at $\omega_0 \approx 1.7$). The analytic solution for κ_f turns out to be (full details are contained in the Supplemental Material [19]) $\kappa_f = (4/\sqrt{1 + (\omega_0/\Delta)^2})$. The latter expression tells us that the critical point for the forward transition is uniquely determined by the dimensionless parameter ω_0/Δ. In particular, when $\omega_0 = 0$, the FD degenerates into the typical unimodal Lorentzian distribution, and $\kappa_f = 4$ is predicted, in full agreement with what is reported in Ref. [3]. Figure 2 gives an account of how remarkably the analytical predictions are verified by numerical simulations (at all values of Δ and within the entire range of ω_0/Δ).

As seen in Fig. 2, κ_f decreases monotonically as ω_0/Δ increases, causing (as $\kappa_b = 2$ always) the hysteresis area to shrink monotonically. When $\omega_0/\Delta = \sqrt{3}$, $\kappa_f = \kappa_b = 2$, and the forward and backward transition points almost coincide [see Fig. 1(c)]. As ω_0/Δ gradually exceeds $\sqrt{3}$, the hysteresis area does not immediately disappear [see the inset of Fig. 1(d)]. Actually, at $\omega_0/\Delta = \sqrt{3}$, a Hopf bifurcation occurs during both the forward and backward processes, and both bifurcations are continuous. For the forward direction, the system first undergoes a continuous transition, followed by an ES transition (as κ further increases). A similar scenario of transitions characterizes also the backward direction. An initial parameter regime $\omega_0/\Delta > \sqrt{3}$ then exists, where the system undergoes the cascade of one continuous and one explosive transition during both forward and backward continuity. A further increase of ω_0/Δ causes the hysteresis area to eventually disappear [Figs. 1(e) and 1(f)], leading to a situation where only continuous transitions occur in the system. It is in this latter regime, i.e., close to a tricritical point in parameter space that novel coherent phases, the *Bellerophon* states, emerge in the path leading the system from its unsynchronized to its synchronized behavior.

The following step involves characterizing such a novel state, and discussing the differences with other typical coherent states of Kuramoto-type models. For the sake of exemplification, we take the case of $\omega_0/\Delta = 3$ [Fig. 1(f)]. Here, the system exhibits two continuous transitions at $\kappa_c^1 = 4/\sqrt{10} \approx 1.26$ and $\kappa_c^2 = 2$, respectively. Therefore, three parameter regimes can be identified: $\kappa < \kappa_c^1$ (I), $\kappa_c^1 < \kappa < \kappa_c^2$ (II), and $\kappa > \kappa_c^2$ (III). In regime I, the coupling strength is small, and the system features the trivial incoherent state. In regime III, the coupling is so strong that the system goes into the fully synchronized state, in which all oscillators split into two fully synchronized clusters. The *Bellerophon* phases are steady states

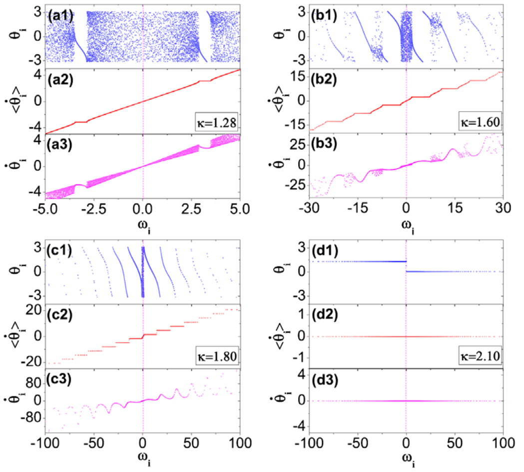

FIG. 3. *Bellerophon* states. Snapshots of the instantaneous phase θ_i (upper plots), the average speed $\langle\dot{\theta}_i\rangle$ (middle plots), and the instantaneous speed $\dot{\theta}_i$ (lower plots) versus the natural frequencies $\{\omega_i\}$ of the oscillators. $\kappa = 1.28$ (a), 1.60 (b), 1.80 (c), and 2.10 (d) (the fully synchronized state). All other parameters are specified in the text. Panels (a)–(c) refer to *Bellerophon* states.

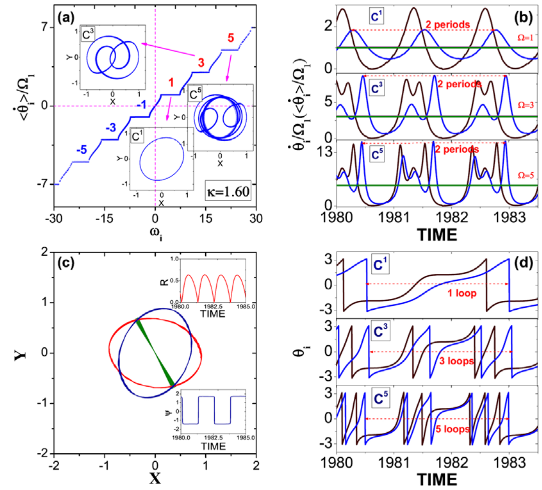

FIG. 4. The state of Fig. 3(b). (a) The average speeds of the coherent clusters. They correspond to odd-numbered multiples of the principle frequency Ω_1. (b) Time series of the instantaneous speeds of the clustered oscillators. In the panel, two sample oscillators are arbitrarily chosen for clusters C^1 (top), C^3 (middle), and C^5 (bottom). The straight lines mark the average speed. (c) Order parameters for all oscillators with positive (blue oval) and negative (red oval) frequency, and order parameter for all oscillators (green lines). The insets are the time series of the global order parameter $R(t)$ and $\Psi(t)$, which are typically oscillatory. (d) Time series of the instantaneous phases corresponding to (b).

occurring in the middle regime II, i.e., during the path to full synchronization. In Fig. 3, four typical phases are illustrated, corresponding to the κ values denoted by letters A, B, C, and D in Fig. 1(f). They are characterized by three quantities: the instantaneous phases θ_i, the instantaneous (angular) speed $\dot{\theta}_i$, and the average speed $\langle\dot{\theta}_i\rangle$ (i.e., the oscillators' effective frequencies), where the bracket stands for a long time average.

In Fig. 3(a), $\kappa = 1.28$. As κ just exceeds $\kappa_c^1 = 1.26$, two small symmetric clusters emerge, whose average speeds are equal to each other in magnitude, but opposite in sign. The oscillators in the two clusters rotate with the same average speed (but different instantaneous phases and frequencies). At $\kappa = 1.60$ [Fig. 3(b)], a multiclustered state emerges. The number of clusters increases in pairs as κ increases, each pair containing oscillators that are symmetric in terms of their natural frequencies. The oscillators inside each cluster have the same average speed [see the staircase structure of Fig. 3(b2)], but different instantaneous frequencies [Fig. 3(b3)]. The clusters coexist with drifting oscillators that are not synchronized. In Fig. 3(c), $\kappa = 1.80$. This is also a *Bellerophon* state, but different from that of Fig. 3(b). The coherent clusters now occupy almost all the range of natural frequencies, except for a small narrow zone around the central frequency; the increase of κ results in all drifting oscillators being gradually recruited into either one of the clusters. Finally, Fig. 3(d) ($\kappa = 2.10$) refers to the fully coherent phase, where two giant clusters are formed. In each cluster, the oscillators with positive or negative frequencies coincide with each other totally: they feature now the same instantaneous speed, so that the whole system behaves like two giant oscillators.

Much better insight is gathered by inspecting the system's macroscopic and microscopic details. Figure 4(a) reveals that the staircases of coherent clusters at $\kappa = 1.60$ satisfy in fact a certain rule: they are quantized, and can be expressed as $\pm(2n-1)\Omega_1$, $n = 1, 2, \ldots,$ [20], where Ω_1 is the lowest frequency, i.e., the principle (or base) system's frequency. Accordingly, depending on their multiple of Ω_1, the clusters can be named $C^1, C^3, C^5, \ldots,$ respectively. The key, and also subtle, point here is that, although the average speeds of the oscillators inside each cluster are equal to each other, their instantaneous speeds are generally different and quite heterogeneous. Furthermore, the instantaneous speeds of the oscillators in each cluster are correlated and form the characteristic cusped pattern [Figs. 3(b3) and 3(c3)] analogous to that featured by the average frequencies of the oscillators within the CS. We emphasize that this similarity is between the instantaneous frequencies in the *Bellerophon* state and the average frequencies in CS. Figure 4(b) shows that the instantaneous speeds of the oscillators inside the same cluster evolve periodically, but different oscillators follow different periodic patterns. In other words, the instantaneous speed for each oscillator evolves uniquely. This makes *Bellerophon* states essentially different with respect to other coherent states observed in Kuramoto-like models, such as the partially coherent state [6], the standing wave state [21,22], the traveling wave state [21,23], and the CS [10,11], where the oscillators inside the coherent cluster are typically frequency locked. Moreover, even though the instantaneous speed of the clusters' oscillators varies nonuniformly during one period (particularly for those clusters with large n), the average speeds during one period for all oscillators in a certain cluster turn out to be the same, i.e., an odd-numbered multiple of Ω_1 in this case. As the instantaneous speed characterizes the rotations of the oscillators along the unit circle, a very interesting collective motion of the oscillators is observed [Fig. 4(d)]: during one period $T_1 = 1/\Omega_1$, the oscillators in C^1 all perform one loop along the unit circle, and in the meantime, the oscillators in C^3 and C^5 rotate three loops and five loops, respectively. In analogy, the oscillators in C^{2n-1} will perform $2n-1$ loops. Compared with Fig. 4(b), we further find that during one loop, the instantaneous speeds for all coherent oscillators experience two periods; i.e., each oscillator repeats its motion during the two half periods. In Fig. 4(a), we report the local value of the order parameter (i.e., that contributed by only those oscillators in a certain cluster) in the complex plane, for C^1, C^3 and C^5. Because of the complicated phase relationships among the oscillators in each cluster [see Fig. 4(d)], the resulting value is typically periodic or quasiperiodic, and follows a complicated orbit. Essentially, each cluster can be seen as a giant oscillator, with properties described by the local order parameter. Figure 4(c) reports the order parameters for all positive and negative frequencies (including the drifting oscillators). In phase space, orbits appear as two smeared ovals, reflecting the quasiperiodic motion of the total order parameter, as shown in the insets of Fig. 4(c). To aid in understanding the *Bellerophon* states' features, the Supplemental Material [19] contains evidence of configurations that include also negative instantaneous phases, together with several animated movies that help visualizing the evolution of the phases, speeds, and motions of the oscillators on the unit circle.

Let us now start to discuss on the conditions needed for the emergence of *Bellerophon* states. First of all, the states appear to be robust under the change of the FD, and in particular under relaxing the hypothesis of a symmetric distribution. Indeed, one can consider the same case (1), but under the choice of an asymmetric Lorentzian distribution. Precisely, $g(\omega)$ is now taken to be $g(\omega) = \Delta/(\pi[(\omega-\omega_0)^2 + \Delta^2])$. When keeping $\Delta = 1$ as a constant, and changing ω_0 (in order to shift the frequency distribution along the positive axis), the typical state that emerges is illustrated in Fig. 5(a).

Furthermore, a correlation between the oscillator's natural frequency and the coupling strength [inherent to case (1)] seems not to be a necessary condition either. One can indeed consider Eq. (1) under case (2), i.e., in the presence of two populations of oscillators, with κ_i only taking two values (either $\kappa_1 < 0$ or $\kappa_2 > 0$). In this case, the natural frequencies $\{\omega_i\}$ are taken from a symmetric distribution centered at zero, the Lorentzian distribution $g(\omega) = \Delta/[\pi(\omega^2 + \Delta^2)]$. Now, the oscillators in the ensemble can be generally divided

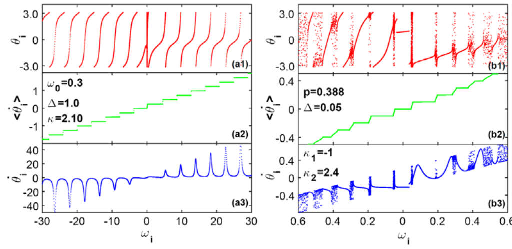

FIG. 5. *Bellerophon* states in different frequency arrangements and models. (a) An asymmetric frequency distribution, and (b) a model including conformists and contrarians. This figure caption is the same as that in Fig. 3, and the legends indicate the values of the used parameters. See the text for the model and frequency specifications.

into two groups: those with positive κ_i (which will behave like conformists attempting to follow the global rhythm of the system), and those with negative κ_i, which will tend to act as contrarians (always trying to oppose the system's global trend) [17]). In numerical simulations, one starts from an incoherent state where only the contrarian oscillators interact, and gradually flips a number of contrarians into conformists. In doing so, various strategies can be adopted as rules for the flipping procedure. Three strategies to change contrarians into conformists have been adopted by us. In strategy (i) contrarians are randomly chosen to be flipped into conformists; in strategy (ii) contrarians are ranked according to the absolute value of their natural frequencies $|\omega_i|$, and then flipped into conformists from the largest $|\omega_i|$ to the smallest, i.e., the coupling strength of the ith oscillators will be $\kappa_i = \kappa_2$ if $|\omega_i| > \omega_0$ and $\kappa_i = \kappa_1$ otherwise. Denote the proportion of conformists in the system as p then $1 - p = \int_{-\omega_0}^{\omega_0} g(\omega)d\omega$; strategy (iii) is the opposite of (ii), i.e., $\kappa_i = \kappa_2$ if $|\omega_i| < \omega_0$ and $\kappa_i = \kappa_1$ otherwise, with $p = \int_{-\omega_0}^{\omega_0} g(\omega)d\omega$. In all the three cases, the emerging scenario is qualitatively the same. While the full analytical treatment of the three cases will be presented elsewhere [24], the numerical results of case (iii) are reported in Fig. 5(b) where one can see that, as the proportion of conformists $p = \int_{-\omega_0}^{\omega_0} g(\omega)d\omega$ increases, the system manifests *Bellerophon* states.

In conclusion, we have provided evidence of a novel, asymptotic, phase of globally coupled oscillators: the *Bellerophon* state, which differs essentially from all coherent phases described so far in coupled oscillator models. Within the novel state, the oscillators form quantized clusters, where neither their phases nor their instantaneous frequencies are locked. The oscillators' instantaneous speeds are different, but they behave periodically, and most importantly, their average speed values are the same. Our results support the hypothesis that *Bellerophon* states are generic, and occur in globally coupled nonidentical oscillators, irrespectively of the symmetric nature of the FD, or of the specific oscillators' coupling scheme. The required condition for the emergence of these states seems to be a model system for which continuous and abrupt transitions to synchronization coexist, in such a way that a setting can be chosen in the relative proximity of the parameter point where the switching in the nature of the synchronization transition (from second-order-like to explosive) occurs. The range of parameters over which the new states are observed turns out to be pretty large, and therefore one actually does not even need to be in the immediate vicinity of such a tricritical point. While revealing functional relationships within each cluster will certainly be a mathematical challenge for the future, our analytical and numerical description will certainly help physicists seek *Bellerophon* states in a variety of experimental and natural systems.

This work was partly supported by the National Natural Science Foundation of China under Grants No. 11305062, No. 11375066, No. 11135001, and No. 11375109, and by the Fundamental Research Funds for the Central Universities under Grant No. GK201303002. We thank Tian Qiu and Wenchang Zhou for assistance.

H. B. and X. H. contributed equally to this work.

*Corresponding author.
stefano.boccaletti@gmail.com
†Corresponding author.
guanshuguang@hotmail.com

[1] Y. Kuramoto, *Chemical Oscillations, Waves and Turbulence* (Springer, New York, 1984).
[2] X. Zhang, X. Hu, J. Kurths, and Z. Liu, Phys. Rev. E **88**, 010802 (2013).
[3] X. Hu, S. Boccaletti, W. Huang, X. Zhang, Z. Liu, S. Guan, and C.-H. Lai, Sci. Rep. **4**, 7262 (2014).
[4] X. Zhang, S. Boccaletti, S. Guan, and Z. Liu, Phys. Rev. Lett. **114**, 038701 (2015).
[5] S. H. Strogatz and R. E. Mirollo, J. Stat. Phys. **63**, 613 (1991).
[6] S. H. Strogatz, Physica (Amsterdam) **143D**, 1 (2000).
[7] D.-S. Lee, Phys. Rev. E **72**, 026208 (2005); S. Guan, X. Wang, Y.-C. Lai, and C.-H. Lai, Phys. Rev. E **77**, 046211 (2008); J. Stout, M. Whiteway, E. Ott, M. Girvan, and T. M. Antonsen, Chaos **21**, 025109 (2011).
[8] Yu. Maistrenko, O. Popovych, O. Burylko, and P. A. Tass, Phys. Rev. Lett. **93**, 084102 (2004); F. De Smet and D. Aeyels, Phys. Rev. E **77**, 066212 (2008); D. Aeyels and F. De Smet, Physica (Amsterdam) **239D**, 1026 (2010).
[9] D. Pazó, Phys. Rev. E **72**, 046211 (2005); J. Gómez-Gardeñes, S. Gómez, A. Arenas, and Y. Moreno, Phys. Rev. Lett. **106**, 128701 (2011); I. Leyva, R. Sevilla-Escoboza, J. M. Buldú, I. Sendiña-Nadal, J. Gómez-Gardeñes, A. Arenas, Y. Moreno, S. Gómez, R. Jaimes-Reátegui, and S. Boccaletti, Phys. Rev. Lett. **108**, 168702 (2012); P. Li, K. Zhang, X. Xu, J. Zhang, and M. Small, Phys. Rev. E **87**, 042803 (2013); I. Leyva, A. Navas, I. Sendiña-Nadal, J. A. Almendral, J. M. Buldú, M. Zanin, D. Papo, and S. Boccaletti, Sci. Rep. **3**, 1281 (2013); I. Leyva, I. Sendiña-Nadal, J. A. Almendral, A. Navas, S. Olmi, and S. Boccaletti, Phys. Rev. E **88**, 042808 (2013).
[10] Y. Kuramoto and D. Battogtokh, Nonlinear Phenom. Complex Syst. **5**, 380 (2002); S.-I. Shima and Y. Kuramoto, Phys. Rev. E **69**, 036213 (2004).
[11] D. M. Abrams and S. H. Strogatz, Phys. Rev. Lett. **93**, 174102 (2004); O. E. Omel'chenko, Y. L. Maistrenko, and P. A. Tass, Phys. Rev. Lett. **100**, 044105 (2008).
[12] M. R. Tinsley, S. Nkomo, and K. Showalter, Nat. Phys. **8**, 662 (2012); A. M. Hagerstrom, T. E. Murphy, R. Roy, P. Hövel, I. Omelchenko, and E. Schöll, Nat. Phys. **8**, 658 (2012); S. Nkomo, M. R. Tinsley, and K. Showalter, Phys. Rev. Lett. **110**, 244102 (2013).
[13] D. M. Abrams, R. Mirollo, S. H. Strogatz, and D. A. Wiley, Phys. Rev. Lett. **101**, 084103 (2008).
[14] G. C. Sethia, A. Sen, and F. M. Atay, Phys. Rev. Lett. **100**, 144102 (2008).
[15] I. Omelchenko, O. E. Omel'chenko, P. Hövel, and E. Schöll, Phys. Rev. Lett. **110**, 224101 (2013).
[16] By specular nature we here mean that the conditions under which the system has to be prepared are exactly the opposite of those giving rise to Chimera states. Chimera states emerge, indeed, for locally coupled identical oscillators, while here one needs globally coupled nonidentical oscillators, and actually our Letter shows that the more different the ensemble's units are, the best is the case for the observation of Bellerophon states.
[17] H. Hong and S. H. Strogatz, Phys. Rev. Lett. **106**, 054102 (2011).
[18] Numerical values are obtained by a fourth order Runge-Kutta integration method, with an integration time step of 0.005. $N = 10000$.
[19] See Supplemental Material at http://link.aps.org/supplemental/10.1103/PhysRevLett.117.204101 for the analytical treatment, characterization of other *Bellerophon* states, and the animated movies.
[20] J. R. Engelbrecht and R. Mirollo, Phys. Rev. Lett. **109**, 034103 (2012).
[21] E. A. Martens, E. Barreto, S. H. Strogatz, E. Ott, P. So, and T. M. Antonsen, Phys. Rev. E **79**, 026204 (2009).
[22] D. Pazó and E. Montbrió, Phys. Rev. E **80**, 046215 (2009).
[23] D. Iatsenko, S. Petkoski, P. V. E. McClintock, and A. Stefanovska, Phys. Rev. Lett. **110**, 064101 (2013).
[24] T. Qiu, S. Boccaletti, I. Bonamassa, Y. Zou, J. Zhou, Z. Liu, and S. Guan, Sci. Rep. **6**, 36713 (2016).